# Formation Kinetics of the Triatomic Excimer Ar$_2$F*

GERD MAROWSKY, GRAHAM P. GLASS, FRANK K. TITTEL, SENIOR MEMBER, IEEE, KRISTIAN HOHLA,
WILLIAM L. WILSON, JR., MEMBER, IEEE, AND H. WEBER

*Abstract*—Detailed fluorescence measurements of electron beam-excited high pressure mixtures of Ar/F$_2$ and Ar/NF$_3$ have been made in order to investigate the processes leading to the formation of Ar$_2$F*. Three-body collisional quenching of ArF* has been identified as a major formation mechanism. The third-order rate constant for this reaction has been measured to be $k_1 = (1.2 \pm 0.2) \times 10^{-30}$ cm$^6 \cdot$ s$^{-1}$. In addition quenching rates for collisional de-excitation of Ar$_2$F* by argon and the fluoride donors NF$_3$ and F$_2$ have been determined. The radiative lifetime has been measured as 219 ± 15 ns. The possible formation of Ar$_2$F* from long-lived excited argon neutrals when using intense excitation densities and low-donor pressures is also briefly discussed.

## I. INTRODUCTION

SINCE the initial characterization of broadband emissions from triatomic rare gas halides [1], [2] and the recent demonstrations of laser action by two electron beam-pumped trimers, Xe$_2$Cl [3], [4] and Kr$_2$F [5], [6], there has been considerable interest in Ar$_2$F as a laser medium. The trimer Ar$_2$F* is of special interest [1], [7]–[17] because its fluorescence covers a broad spectral range in the UV centered at 285 ± 25 nm, a region that is currently not obtainable via single step coherent processes. Another reason for the interest is the relative simplicity of the argon-halogen donor system, as argon can be used both as a buffer gas for efficient electron-beam energy deposition and as an active medium for Ar$_2$F* production. However, due to the low cross section for stimulated emission [4] and the large Ar$_2^+$ and Ar$_2^*$ absorptions [18]–[20] which spectrally overlap the fluorescence, no Ar$_2$F laser action has as yet been observed. In the present paper, the procedures developed for the study of Xe$_2$Cl production and quenching [21] are utilized in order to obtain a better understanding of the kinetic processes leading to the formation of Ar$_2$F* following electron beam excitation of Ar/F$_2$ and Ar/NF$_3$ mixtures.

## II. EXPERIMENTAL APPARATUS AND TECHNIQUES

Details of the electron-beam apparatus used for most the experiments discussed in this paper have been described elsewhere [3], [4]. Therefore, the description given below is

limited to details specific to the study of Ar$_2$F*. Mixtures of high purity argon (0.5–6 atm) and the halogen donor (0.5–20 torr of pure NF$_3$ or of 10 percent F$_2$ in He) were irradiated by an intense electron beam, produced by a Pulserad 110 accelerator (1 MeV, 15 kA) having a typical pulse duration of 8–10 ns. Great care was taken to keep the reaction cell as clean as possible. The gas mixture was replaced after every shot. In addition, the most critical data were obtained only after a long pumping of the reaction cell under high vacuum conditions. The ArF* emission was little affected by cell purity. However, due to its long lifetime, the Ar$_2$F* emission was far more sensitive to contaminants and the intensity decreased by as much as a factor of two unless the cell was properly purged.

A few experiments were performed using a coaxial field emission diode [22], [23] instead of a transverse electron beam pump geometry [3], [4]. The diode was fed either with a Pulserad 110A accelerator (1.3 MeV, 12 kA, 20 ns) or a Febetron 706 (600 keV, 5 kA, 2 ns). This method of pumping resulted in extremely high excitation densities in the Ar–F$_2$/NF$_3$ mixtures of ~300 MW/cm$^2$.

Time-integrated fluorescence spectra were obtained using an optical multichannel analyzer (OMA). A typical spectrum consisting of a narrow ArF*($B \rightarrow X$) transition and a broad-band Ar$_2$F* emission, which became more prominent at higher argon pressures, is shown in Fig. 1. In this figure, the relative total intensities corrected for the OMA spectral response are in the ratio 1:32. Time-resolved measurements were made using a fast vacuum photodiode coupled to a transient digitizer, which itself was interfaced to a DEC PDP 11/23 minicomputer system. Appropriate filters were used to select the narrow ArF* emission centered at 193 nm or the broadband Ar$_2$F* fluorescence at 285 nm. Data reduction to yield either a time-integrated photodiode signal or an exponential decay constant was performed using computer routines developed previously [21], [24].

## III. RESULTS AND ANALYSIS

Since the fluorescence emitted by Ar$_2$F* was generally observed to reach its peak value only after that emitted by ArF* had effectively decayed to zero, a formation mechanism involving ArF* as a precursor of Ar$_2$F* was first considered. The third-order quenching reaction of ArF*

$$\text{ArF*} + \text{Ar} + \text{Ar} \rightarrow \text{Ar}_2\text{F*} + \text{Ar} \qquad (1)$$

has been proposed previously [7], [10], [11] as a possible mechanism for the formation of Ar$_2$F*. If such a reaction occurs, then it can be shown (see [21, equations (10)–(12)]) that the total time-integrated fluorescence emitted at 285 nm by Ar$_2$F*, $\int I_{285} \, dt$, is related to that emitted at 193 nm by ArF*, $\int I_{193} \, dt$, by the equation
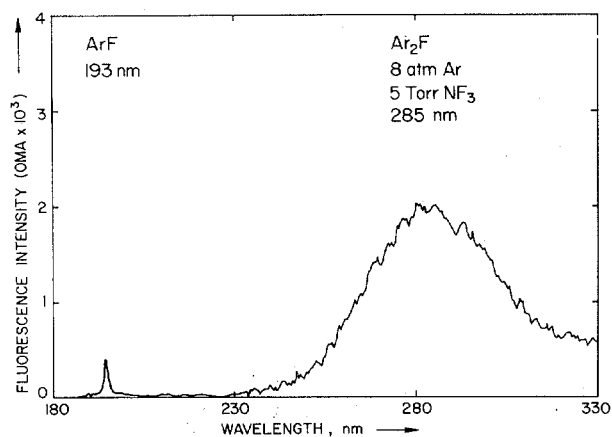
Fig. 1. Fluorescence spectrum of electron beam-excited $Ar-NF_3$ mixture depicting both the $B \to X$ transition of $ArF^*$ and the broad-band emission of $Ar_2F^*$.

$$\int I_{285} \ dt \bigg/ \int I_{193} \ dt = k_1 (Ar)^2 \ \tau[\tau_{193}/\tau_{285}] \qquad (2)$$

where $k_1$ is the termolecular rate constant for reaction (1), (Ar) is the particle density of argon in $cm^{-3}$, $\tau_{193}$ and $\tau_{285}$ are the radiative lifetimes of $ArF^*$ and $Ar_2F^*$, respectively, and $\tau$ is the effective exponential decay constant for $Ar_2F^*$ given by the expression

$$\tau^{-1} = \tau_{285}^{-1} + k_{Ar}^q(Ar) + k_{F_2}^q(F_2). \qquad (3)$$

Here, $k_{Ar}^q$ and $k_{F_2}^q$ are rate constants for the two-body collisional quenching of $Ar_2F^*$ by Ar and the fluorine donor (here considered to be $F_2$), respectively.

Fig. 2 displays the experimentally measured fluorescence ratio ($\int I_{285} \ dt / \int I_{193} \ dt$) as a function of the square of the argon partial pressure for a number of mixtures, all containing a fixed amount of 3 torr of $F_2$. The effective decay constant $\tau$ did not change as the argon pressure was varied, being measured as $38 \pm 3$ ns. Therefore, the linearity of the plot strongly suggests that $Ar_2F^*$ was formed primarily via three-body quenching of $ArF^*$. The rate constant for reaction (1) was determined from the slope of Fig. 2, using (2), to be

$$k_1 = (1.2 \pm 0.2) \times 10^{-30} \ cm^6 \cdot s^{-1}.$$

In making this determination the radiative lifetime of $Ar_2F^*$ was taken to be 219 ns, the value measured in this work, and the radiative lifetime of $ArF^*$ was taken to be 4 ns, the value calculated by Dunning and Hay [25].

The value of $k_1$ is somewhat higher than the values previously published [7], [10]-[12]. However, our value depends inversely on $\tau_{193}$, and recent experimental evidence suggests that the calculated radiative lifetime may be too low [26]. The uncertainty in $k_1$ is somewhat higher than the quoted standard deviation. It arises largely from the problem of accurately comparing the photodiode-filter combination response at 193 and 285 nm.

The rate of collisional quenching of $Ar_2F^*$ by $F_2$ (and by $NF_3$) was established by monitoring $I_{285}$ *after* $I_{193}$ had effectively decayed to zero. The decay constant $\tau$ for $Ar_2F^*$ was measured for a number of mixtures containing a constant amount of argon (chosen to be 2 atm in one series of measurements and 6 atm in another), but different amounts of $F_2$ (or
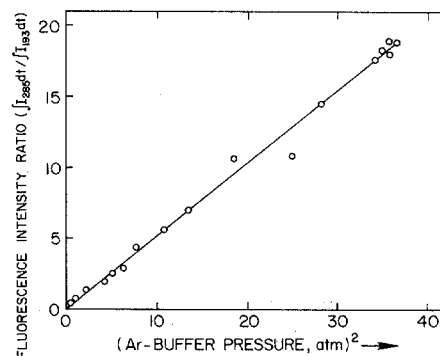


Fig. 2. The ratio of total time integrated fluorescence emitted by $Ar_2F^*$ at 285 nm to that emitted by $ArF^*$ at 193 nm plotted against the square of the argon buffer gas pressure. All mixtures contained a fixed amount of 3 torr of $F_2$.
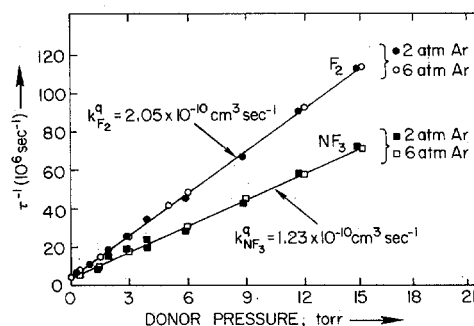


Fig. 3. Stern-Volmer plots for $Ar_2F^*$. The fluorescence decay frequency is plotted versus the partial pressure of either $F_2$ or $NF_3$ for mixtures containing either 2 atm argon (solid points) or 6 atm argon (open points).

$NF_3$). Some of the experimental data is displayed in Fig. 3. As can be seen from these Stern-Volmer plots, data taken in the presence of 2 atm of argon were indistinguishable from those taken in the presence of 6 atm of argon. Therefore, an upper limit of $10^{-14} \ cm^3 \cdot s^{-1}$ could be assigned to $k_{Ar}^q$, the rate constant for quenching of $Ar_2F^*$ by argon. The rate constants for collisional quenching of $Ar_2F^*$ by $F_2$ and $NF_3$ were calculated from the slopes of the appropriate Stern-Volmer plots using (3), as

$$k_{F_2}^q = (2.05 \pm 0.06) \times 10^{-10} \ cm^3 \cdot s^{-1}$$

and

$$k_{NF_3}^q = (1.23 \pm 0.05) \times 10^{-10} \ cm^3 \cdot s^{-1},$$

respectively. The radiative lifetime of $Ar_2F^*$ was determined by extrapolating the measured decay frequencies to zero donor pressure as
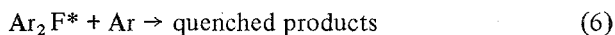
$$\tau_{285} = 219 \pm 15 \ ns.$$

This value may be compared to the value of 185 ns reported in [7]-[9]. The lower quenching rate observed when using $NF_3$ is consistent with the behavior observed in [27] for the quenching of $Kr_2F^*$ by $F_2$ and $NF_3$.

Although the data presented in Fig. 2 suggest that $Ar_2F^*$ is formed primarily as a result of three-body quenching of $ArF^*$, a number of experiments and calculations were performed in order to further check this hypothesis. The experiments involved adding up to 10 torr of $SF_6$ to the reaction mixtures prior to electron beam excitation. $SF_6$ is known to possess a

large electron capture cross section [28] and is known to strongly inhibit the dissociative attachment reaction that leads to the formation of excited neutrals subsequent to electron beam excitation of argon [29].

$$Ar_2^+ + e \rightarrow Ar^* + Ar. \tag{4}$$

Previous studies with transverse electron beam pumping have shown that the addition of 1 torr of $SF_6$ greatly decreases the formation of the $N_2(C)$ state which is produced by excitation transfer from $Ar^*$ in electron beam excited $Ar/N_2$ mixtures [30]. In the present study, the addition of $SF_6$ had little effect on either the yield or the temporal behavior of $Ar_2F^*$. Therefore, it may be concluded that under the conditions of this study, excited neutrals such as $Ar^*$ and $Ar_2^*$ play an insignificant role in the production of $Ar_2F^*$. The calculations involved numerical integration of the rate equations pertinent to the formation and removal of $Ar_2F^*$ via the following model:

$$ArF^* + Ar + Ar \rightarrow Ar_2F^* + Ar \tag{1}$$

$$Ar_2F^* + F_2 \rightarrow \text{quenched products} \tag{5}$$

$$Ar_2F^* + Ar \rightarrow \text{quenched products} \tag{6}$$

$$Ar_2F^* \rightarrow 2Ar + F + h\nu. \tag{7}$$
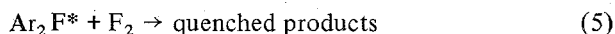
The integration was performed using Euler's method with a stepsize of $\sim4 \times 10^{-11}$ s. The concentration of $ArF^*$ was calculated from the intensity of the experimentally measured $ArF(B \rightarrow X)$ fluorescence and was used as input data into the calculation. This input took the form of an array of 512 successive intensity measurements recorded on a transient digitizer over a time interval of 200 ns. The radiative lifetime of $Ar_2F^*$ was taken to be 219 ns, and the rate constants for the quenching reactions were chosen to be $k_5 \equiv k_{F_2}^q = 2.05 \times 10^{-10}$ cm$^3 \cdot$ s$^{-1}$, and $k_6 \equiv k_{Ar}^q = 10^{-14}$ cm$^3 \cdot$ s$^{-1}$ in order to fit the decay measurements previously discussed. The third-order rate constant $k_1$ was initially chosen to be $1.2 \times 10^{-30}$ cm$^6 \cdot$ s$^{-1}$, but this constant was later varied slightly in order to provide a "best fit" between experiment and calculation.

Temporal profiles of $Ar_2F^*$ fluorescence were calculated for a variety of mixtures containing 3 torr $F_2$ and varying amounts of argon ranging from 1-6 atm. A typical comparison between a calculation and an experiment is shown in Fig. 4. Equally good comparisons were obtained for the other mixtures studied. The overall degree of agreement between computation and experiment confirms the validity of the proposed $Ar_2F^*$ formation mechanism in these experiments.

Although $Ar_2F^*$ formation via three-body quenching of $ArF^*$ may be considered as the dominant pathway when operating under the conditions described above, other experiments performed using higher argon and lower $F_2$ pressures and more intense electron beam excitation have shown that other formation pathways can sometimes also be important. For instance, when using the higher primary electron densities that can be achieved by coaxial pumping, the temporal profile of $Ar_2F^*$ fluorescence emitted by a mixture containing 1 torr $F_2$ and 6 atm argon contained two temporal components as shown in Fig. 5. The initial component can be readily identified as being produced from a short-lived $ArF^*$ intermedi-
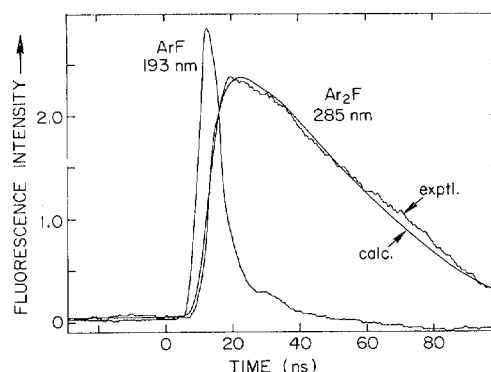


Fig. 4. Observed and calculated time dependence of $Ar_2F^*$ fluorescence emitted for a mixture containing 3 torr $F_2$ and 2 atm argon. The calculated profile used kinetic data presented in the text, with $k_1$ chosen to be $1.33 \times 10^{-30}$ cm$^6 \cdot$ s$^{-1}$.
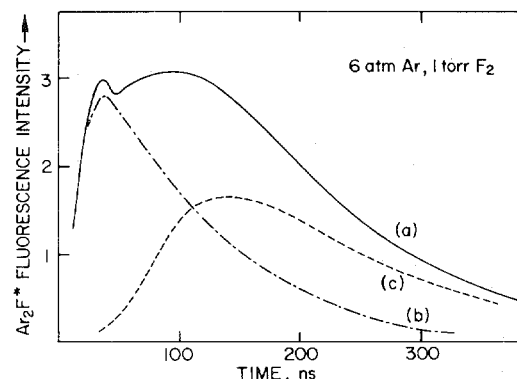


Fig. 5. Temporal fluorescence characteristics of a coaxially pumped $Ar-F_2$ mixture depicting two distinct formations channels for $Ar_2F^*$ (a) experimental $Ar_2F^*$ temporal behavior, (b) computed profile of $Ar_2F^*$ formed via three-body quenching of $ArF^*$, (c) the curve obtained by subtraction of (b) from (a), showing a delayed component that is probably produced by long-lived argon species.

ate. In fact, the dashed line labeled (b) in this figure can be synthesized directly from the observed $ArF^*$ fluorescence using the rate constants for the formation reaction (1) and the quenching reactions (5), (6), and (7) described above. The remaining contribution, labeled in Fig. 5 as peak (c), arises from an entirely different $Ar_2F^*$ formation mechanism. The relative contributions from the two mechanisms change as the total pressure is altered. At low argon pressures (1 atm), the temporal profile of the overall fluorescence resembles curve (b), and $Ar_2F^*$ production is dominated by the three-body reaction with $ArF^*$. At higher pressures (16 atm), the overall fluorescence resembles curve (c), and $Ar_2F^*$ production occurs largely by the other mechanism. Furthermore, as a result of this second formation mechanism, the argon pressure dependence of the $Ar_2F^*$ fluorescence emitted subsequent to coaxial pumping is quite different from that emitted following transverse electron beam excitation, as can be seen in Fig. 6.

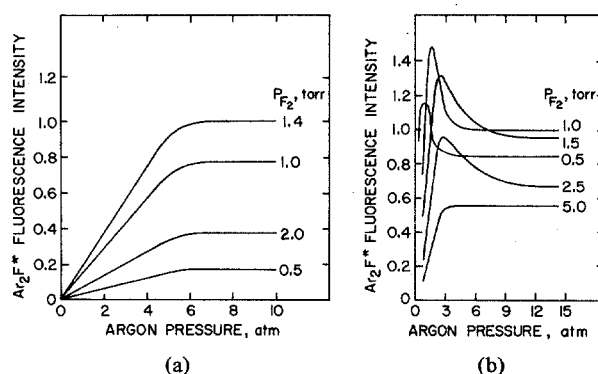A reasonable explanation for this behavior can be obtained by considering the following mechanism:

$$e_f + Ar \rightarrow e_f + Ar^+ + e_s \tag{8}$$

$$e_s + F_2 \rightarrow F^- + F \tag{9}$$

$$Ar^+ + F^- \rightarrow ArF^* \tag{10}$$

$$ArF^* + Ar + Ar \rightarrow Ar_2F^* + Ar. \tag{1}$$

Fig. 6. Comparison of Ar pressure dependence of Ar$_2$F* fluorescence for (a) transverse $e$-beam excitation and (b) coaxial $e$-beam excitation of argon-F$_2$ mixtures at various F$_2$ pressures.

TABLE I
SUMMARY OF Ar$_2$F* RATE CONSTANTS

| Reaction | Rate Constant | Other Work |
|---|---|---|
| 1) ArF* + Ar + Ar → Ar$_2$F* + Ar | $k_1 = (1.2 \pm 0.2) \times 10^{-30} cm^6 s^{-1}$ | $0.6 \times 10^{-30}$ [12], $0.4 \times 10^{-30}$ [11], $0.5 \times 10^{-30} cm^6 s^{-1}$ [7,9,16] |
| 2) Ar$_2$F* → 2Ar + F + h$\nu$ (285 nm) | $\tau_{285} = 219 \pm 15$ ns | 185 ns [7-9], 230 ns [16] |
| 3) Ar$_2$F* + F$_2$ → quenching | $k^q_{F_2} = (2.05 \pm 0.06) \times 10^{-10} cm^3 s^{-1}$ | $2.1 \times 10^{-10} cm^3 s^{-1}$ [9] |
| 4) Ar$_2$F* + NF$_3$ → quenching | $k^q_{NF_3} = (1.23 \pm 0.05) \times 10^{-10} cm^3 s^{-1}$ | $5.6 \times 10^{-10} cm^3 s^{-1}$ [16] |
| 5) Ar$_2$F* + Ar → quenching | $k^q_{Ar} < 10^{-14} cm^3 s^{-1}$ | $2.2 \times 10^{-14} cm^3 s^{-1}$ [16] |

Here $e_f$ represents fast 1 MeV electrons that deposit energy into the buffer gas, producing argon ions and secondary electrons. A relatively small number of secondary electron ($e_s$) are produced when using the lower primary beam intensities using the transverse electron beam configuration or when operating at low argon pressures. These secondary electrons are largely captured by F$_2$ in reaction (9), producing F$^-$, and thus Ar$_2$F* via reactions (10) and (1). However, when higher electron beam intensities and higher argon pressures are used, more secondary electrons are produced. If the density of F$_2$ is kept low, many of these remain unattached, and therefore participate in the following sequence which produces long-lived argon neutrals.

$$Ar^+ + Ar + Ar \rightarrow Ar_2^+ + Ar \qquad (11)$$

$$Ar_2^+ + e_s \rightarrow Ar^* + Ar \qquad (12)$$

$$Ar^* + Ar + Ar \rightarrow Ar_2^* + Ar. \qquad (13)$$

Some of these long-lived species may be precursors of the delayed Ar$_2$F* fluorescence shown in Fig. 5.

## IV. CONCLUSIONS

When using moderate electron beam intensities, low buffer gas pressure, and high fluorescence donor concentrations, Ar$_2$F* is formed primarily via a three-body reaction involving ArF*. Rate constants for the reaction producing Ar$_2$F*, and for various reactions removing it from the system are given in Table I. At high $e$-beam intensities and low fluorine donor pressures, other mechanisms producing Ar$_2$F* become prominent.

REFERENCES

[1] D. C. Lorents, D. L. Huestis, M. V. McCusker, H. H. Nakano, and R. M. Hill, "Optical emissions of triatomic rare gas halides," *J. Chem. Phys.*, vol. 68, pp. 4657-4661, 1978.
[2] D. L. Huestis, R. M. Hill, D. J. Eckstrom, M. V. McCusker, D. C. Lorents, H. H. Nakano, B. E. Perry, J. A. Margevicius, and N. E. Schlotter, "New electronic transition laser systems," SRI Int., Menlo Park, CA, SRI Project PYU-1658, Tech. Rep. 1, 1978.
[3] F. K. Tittel, W. L. Wilson, R. E. Stickel, G. Marowsky, and W. E. Ernst, "A triatomic Xe$_2$Cl excimer laser in the visible," *Appl. Phys. Lett.*, vol. 36, pp. 405-407, 1980.
[4] F. K. Tittel, G. Marowsky, W. L. Wilson, and M. C. Smayling, "Electron beam pumped broadband diatomic and triatomic excimer lasers," *IEEE J. Quantum Electron.*, vol. QE-17, pp. 2268-2281, Dec. 1981.
[5] F. K. Tittel, G. Marowsky, M. C. Smayling, and W. L. Wilson, "Blue laser action by the rare-gas halide trimer Kr$_2$F," *Appl. Phys. Lett.*, vol. 37, pp. 862-864, 1981.
[6] N. G. Basov, V. S. Zuev, A. V. Kanaev, L. D. Mikheev, and D. B. Stavrovsky, "Laser action in an optically pumped Kr$_2$F triatomic excimer," *Sov. J. Quantum Electron.*, vol. 7, pp. 2660-2661, 1980.
[7] C. H. Chen, M. G. Payne, and J. P. Judish, "Kinetic studies of ArF* and Ar$_2$F* in proton excited Ar-F$_2$ mixtures," *J. Chem. Phys.*, vol. 69, pp. 1626-1635, 1978.
[8] C. H. Chen and M. G. Payne, "Ar$_2$F radiative lifetime measurement," *Appl. Phys. Lett.*, vol. 32, pp. 358-360, 1978.
[9] —, "Kinetics of proton-excited Ar-F$_2$ and Kr-F$_2$ mixtures," *IEEE J. Quantum Electron.*, vol. QE-15, pp. 149-161, 1979.
[10] M. Rokni, J. H. Jacob, and J. A. Mangano, "Absorption in Ne and Ar rich XeF laser mixtures," *Appl. Phys. Lett.*, vol. 32, pp. 622-624, 1978.
[11] —, "Dominant formation and quenching processes in E beam pumped ArF* and KrF* lasers," *Phys. Rev.*, vol. 16A, pp. 2216-2223, 1977.
[12] V. H. Shui and C. Duzy, "Theoretical study of the formation rates of rare-gas halide trimers," *Appl. Phys. Lett.*, vol. 36, pp. 135-136, 1980.
[13] H. H. Michels, R. H. Hobbs, and L. A. Wright, "The electronic

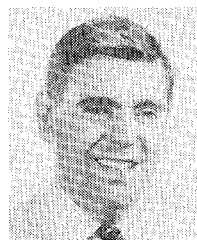structure of ArF and $Ar_2F$," *Chem. Phys. Lett.*, vol. 48, pp. 158-161, 1977.

[14] W. R. Wadt and P. J. Hay, "Electronic states of $Ar_2F$ and $Kr_2F$," *J. Chem. Phys.*, vol. 68, pp. 3850-3863, 1978.

[15] N. G. Basov, V. A. Danilychev, V. A. Dolgikh, O. M. Kerimov, V. S. Lebedev, and A. G. Molchauou, "Kinetics of excimer formation in lasers utilizing rare gas-fluorine mixtures," *Sov. J. Quantum Electron.*, vol. 9, pp. 593-597, 1979.

[16] N. Boewering, R. Sauerbrey, and H. Langhoff, "Kinetic studies of $Ar_2F^*$ in electron beam excited $Ar-NF_3$ mixtures," to be published.

[17] K. S. Jancaitis and H. T. Powell, "Selection and radiative quenching of $Ar_2F$ and $Kr_2F$," presented at the 34th Annu. Gas. Electron. Conf., Boston, MA, Oct. 19-23, 1981.

[18] J. J. Ewing, "Excimer lasers," in *Lasers Handbook*, vol. 3. New York: North-Holland, 1979.

[19] H. H. Michels, R. H. Hobbs, and L. A. Wright, "Electronic structure of the noble gas dimer ions, part II," *J. Chem. Phys.*, vol. 71, pp. 5053-5062, 1979.

[20] F. Collier, J. B. Leblonel, F. Hoffbeck, and P. Cottin, "UV transient absorptions in high pressure argon excited by relativistic electrons," *J. Chem. Phys.*, vol. 74, pp. 4372-4379, 1981.

[21] G. Marowsky, G. P. Glass, M. C. Smayling, F. K. Tittel, and W. L. Wilson, "Dominant formation and quenching kinetics of electron beam pumped $Xe_2Cl$," *J. Chem. Phys.*, vol. 75, pp. 1153-1158, 1981.

[22] M. Diegelmann, W. G. Wrobel, and K. Hohla, "Time-resolved spectroscopy of the $Ar_2^*$ excimer emission," *Appl. Phys. Lett.*, vol. 33, pp. 525-527, 1978.

[23] W. B. Wrobel, H. Rohr, and K. Steuer, "Tunable vacuum UV laser action by argon excimers," *Appl. Phys. Lett.*, vol. 36, pp. 113-115, 1980.

[24] G. P. Glass, F. K. Tittel, W. L. Wilson, Jr., M. C. Smayling, and G. Marowsky, "Quenching kinetics of electron beam pumped XeCl," *Chem. Phys. Lett.*, vol. 83, pp. 585-589, 1981.

[25] T. H. Dunning and P. J. Hay, "The covalent and ionic states of the rare gas monofluorides," *J. Chem. Phys.*, vol. 69, pp. 134-149, 1978.

[26] C. Chen, unpublished work and preliminary experimental observations when using 2 ns long Febatron 706 pump pulse.

[27] M. C. Smayling, Ph.D. dissertation, Rice Univ., Houston, TX.

[28] L. G. Christophorou, D. L. McCorkle, and J. G. Carter, "Cross-section for electron attachment and resonances peaking at sub-thermal energies," *J. Chem. Phys.*, vol. 54, pp. 253-260, 1971.

[29] J. G. Calve and M. Bourene, "Pulse radiolysis of argon-nitrogen mixtures," *J. Chem. Phys.*, vol. 58, pp. 1446-1451, 1973.

[30] G. Marowsky, G. P. Glass, F. K. Tittel, and W. L. Wilson, Jr., "Energy transfer from electron-beam excited argon to nitrogen and POPOP dye vapor," *Chem. Phys. Lett.*, vol. 67, pp. 243-247, 1979.

**Graham P. Glass** was born in Birmingham, England, on July 21, 1938. He received the B.Sc. degree in chemistry from Birmingham University, England, in 1959, and the Ph.D. degree in physical chemistry from Cambridge University, Cambridge, England, in 1963.

After serving as a Postdoctoral Research Associate at Harvard University, Cambridge, MA, he joined the faculty of Essex University, England, in 1965. In 1967 he began an appointment at Rice University, Houston, TX, where he is currently serving as Associate Professor of Chemistry. His research interests include the study of high temperature combustion chemistry using shock waves, fast free radical reactions using EPR, and energy transfer processes using chemical lasers.

Dr. Glass is a member of the American Chemical Society and the American Physical Society.
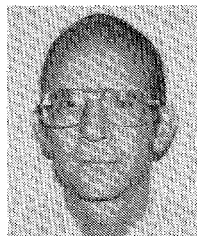
**Frank K. Tittel** (SM'72) was born in Berlin, Germany, in 1933. He received the M.A. and Ph.D. degrees in physics from Oxford University, Oxford, England.

From 1959 to 1967 he was a Research Physicist at the General Electric Research and Development Center, Schenectady, NY. Since 1967 he has been at Rice University, Houston, TX, where he is a Professor of Electrical Engineering. His research interests include laser devices, laser spectroscopy and nonlinear optics.

Dr. Tittel is a member of the Optical Society of America and the American Physical Society.

**Kristian Hohla** was born in Prag, on June 11, 1943. He received the Diplom-degree and the Ph.D. degree in physics from the University of Munich, Munich, Germany, in 1968 and 1971, respectively.

From 1970 to 1975 he worked at the Institut for Plasmaphysik on high power lasers (iodine lasers) and from 1975 to 1980 at the Max-Planck Institut for Quantenoptik on new UV lasers and their application. From 1980 to 1981 he was with the Los Alamos National Laboratory and the University of Illinois at Chicago Circle working on free electron lasers and VUV sources. Since 1981 he has been with Lambda Physik, Göttingen, Germany, as Director of the Research and Development Division.

**Gerd Marowsky** was born in Offenbach am Main, Germany, on December 14, 1939. He received the Diploma in physics from the Technische Hochschule Darmstadt, Darmstadt, Germany, in 1966, and the Ph.D. degree from the University of Göttingen, Göttingen, Germany, in 1969.

From 1969 to 1970 he was a Postdoctoral Fellow at the Institut für Radiochemie at the Kernforschungsanlage Jülich, Germany. In 1970 he joined Carl Zeiss, Oberkochen, to continue work on trace analysis using optical methods, especially fluorescence analysis with dye lasers. Since 1971 he has been with the Laser Group at the Max-Planck-Institut für Biophysikalische Chemie, Göttingen, Germany, where he is involved in the development of novel dye lasers, such as electron-beam pumped organic dyes in the vapor phase.

Dr. Marowsky is a member of the German Physical Society.

**William L. Wilson, Jr.** (S'68-M'71) was born in Bay Shore, NY, on February 6, 1943. He received the B.S. degree in 1965, the M.E.E. degree in 1966, and the Ph.D. degree in 1972, all in electrical engineering from Cornell University, Ithaca, NY.

From 1971 to 1972 he was an Instructor-Research Associate with the Department of Electrical Engineering, Cornell. In 1972 he became an Assistant Professor of Electrical Engineering at Rice University, Houston, TX, where he is currently an Associate Professor. His research interests include infrared and far-infrared devices, as well as excimer lasers. He has also worked on thin-film magnetic devices and solid-state microwave devices.

Dr. Wilson is a member of Tau Beta Pi, Eta Kappa Nu, Sigma Xi, the IEEE Magnetics, Electron Devices, and Microwave Theory and Techniques Societies and the IEEE Quantum Electronics and Applications Society.

**H. Weber**, photograph and biography not available at the time of publication.